the motion of the matrix unlabeled chains is frozen (half-filled symbols).[9] In the insert the same data are reported as a function of the number of entanglements along the test chain, $N/g \sim (\phi/\phi^*)^x$, with $x = -5/4$ for good solvent and $x = -2$ for Θ solvent. We do not expect exactly the same scaling law for the two solvents due to the different molecular weight dependences of D_0, but the fact that the data points fall very close in good and Θ solvent gives a good illustration of the fact that the relevant parameter for self-diffusion is the number of topological constraints imposed on the test chain by its neighbors.

Conclusion

Using the forced Rayleigh light scattering technique, we have measured the self-diffusion coefficient of polystyrene chains in cyclopentane at the Θ temperature. Both the molecular weight and the concentration dependences we obtain are in good agreement with a description of semidilute Θ solutions based on reptation and scaling ideas: (i) the M^{-2} behavior and the weak dependence of D_{self} on the molecular weight of the unlabeled chains are characteristic of a reptative process; (ii) the c^{-3} dependence can be interpreted by assuming that the virtual tube inside which each test chain is confined by its neighbors has a width proportional to the average distance between ternary monomer contacts, $\xi \sim c^{-1}$. This seems a priori surprising: one is used to thinking of tube width in terms of average distance between binary monomer contact points, as the chains cannot cross each other. However, a careful analysis of the description of entangled Θ systems proposed by Brochard and de Gennes shows that this results from the fact that, on the average, all the monomers contained in one subunit of size ξ pertain to the same chain. As far as we are dealing with slow macroscopic motions (i.e., over distances greater than the chain radius), our results show that semidilute Θ systems obey simple scaling laws very similar to those of the good solvent case.

Registry No. Polystyrene, 9003-53-6; cyclopentane, 287-92-3.

References and Notes

(1) de Gennes, P.-G.; Lêger, L. *Annu. Rev. Phys. Chem.* **1982**, *33*, 49.
(2) Lêger, L.; Hervet, H.; Rondelez, F. *Macromolecules* **1981**, *14*, 1732.
(3) Callaghan, P. T.; Pinder, D. N. *Macromolecules* **1980**, *13*, 1085. Callaghan, P. T.; Pinder, D. N. *Macromolecules* **1981**, *14*, 1334.
(4) Tanner, J. E. *Macromolecules* **1971**, *4*, 748.
(5) Klein, J.; Briscoe, B. J. *Proc. R. Soc. London Ser. A*, **1979**, *365*, 53.
(6) Hanley, B.; Balloge, S.; Tirrell, M. *Chem. Eng. Commun.* **1983**, *24*, 93.
(7) Martin, J. E. *Macromolecules* **1984**, *17*, 1279.
(8) Bartels, C. R.; Crist, B.; Graessley, W. W. *Macromolecules* **1984**, *17*, 2702.
(9) Marmonier, M. F.; Lêger, L. *Phys. Rev. Lett.* **1985**, *55*, 1078.
(10) de Gennes, P.-G. *J. Chem. Phys.* **1971**, *55*, 572.
(11) de Gennes, P.-G. *Scaling Concepts in Polymer Physics*; Cornell University: Ithaca, NY, 1979.
(12) de Gennes, P.-G. *Macromolecules* **1976**, *9*, 594.
(13) Brochard, F.; de Gennes, P.-G. *Macromolecules* **1977**, *10*, 1157.
(14) Brochard, F. *J. Phys. (Les Ulis, Fr.)* **1983**, *44*, 39.
(15) Amis, E. J.; Han, C.; Matsushita, Y. *Polymer* **1984**, *25*, 650.
(16) Balloge, S.; Tirrell, M. *Macromolecules* **1985**, *18*, 817.
(17) Wesson, J. A.; Noh, I.; Kitano, T.; Yu, H. *Macromolecules* **1984**, *17*, 782.
(18) Johnson, C. S. *J. Opt. Soc. Am.* **1985**, *B2*, 317.
(19) Eichler, H.; Saije, G.; Stahl, H. *Appl. Phys.* **1973**, *44*, 5383.
(20) Phol, D. W.; Schwatz, S. E.; Irniger, V. *Phys. Rev. Lett.* **1973**, *31*, 32.
(21) Nelson, K. A.; Casalegno, R.; Bwagne-Miller, R. J.; Fayer, M. D. *J. Chem. Phys.* **1982**, *77*, 1144.
(22) Glass, A. H. In *Photonics*; Balkanski, H., Lallemand, P., Eds.; Gauthier-Villars: Paris, 1975.
(23) Irie, M.; Tanaka, H. *Macromolecules* **1983**, *16*, 210. Menju, A.; Hayashi, K.; Irie, M. *Macromolecules* **1981**, *14*, 755.
(24) Green, P. F.; Mills, P. J.; Palmstrøm, C. J.; Mayer, J. W.; Kramer, E. J. *Phys. Rev. Lett.* **1984**, *53*, 2145.
(25) Smith, B. A.; Samulski, E. T.; Yu, L. P.; Winnik, M. A. *Phys. Rev. Lett.* **1984**, *52*, 45.
(26) Adam, M.; Delsanti, M. *Macromolecules* **1985**, *18*, 1760.
(27) Daoud, M.; de Gennes, P.-G. *J. Polym. Sci., Polym. Phys. Ed.* **1979**, *17*, 1981.
(28) Vidakovic, P.; Allain, C.; Rondelez, F. *J. Phys., Lett.* **1981**, *42*, L-323.
(29) Pouyet, G.; Candau, F.; Dayantis, J. *Makromol. Chem.* **1976**, *177*, 2973.

Upper and Lower Critical Solution Temperature Behavior in Thermoplastic Polymer Blends

Guangmin Cong,† Yuhui Huang,† William J. MacKnight,* and Frank E. Karasz

Polymer Science and Engineering Department, University of Massachusetts, Amherst, Massachusetts 01003.

Received March 3, 1986

ABSTRACT: The phase behavior of blends of polystyrene ($\bar{M}_w$ = 115 000, M_w/M_n < 1.06) (PS_{115}) and a random copolymer of carboxylated poly(2,6-dimethyl-1,4-phenylene oxide) (C^y-PPO) has been studied by differential scanning calorimetry (DSC) and light scattering. In C^y-PPO, y represents the carboxyl content (COOH mole percent). The phase diagrams of $C^{8.0}PPO/PS_{115}$ and $C^{10.3}PPO/PS_{115}$ were found to exhibit both UCST (upper critical solution temperature) and LCST (lower critical solution temperature) behavior. The phase behavior is reversible. The miscible region between the UCST and LCST decreases with increasing carboxyl content in the C-PPO, and the critical point moves to lower mass fraction of copolymer. In the blends $C^{4.5}$-PPO/PS_{115} and $C^{6.7}$-PPO/PS_{115} no phase separation was observed during thermal treatment. The results obtained from both DSC and light scattering are consistent.

Introduction

The phase behavior of solutions at constant pressure and temperature is governed by the Gibbs free energy of mixing ΔG_m:

$$\Delta G_m = \Delta H_m - T\Delta S_m \quad (1)$$

Using the Flory–Huggins theory,[1] one may write the entropy of mixing ΔS_m as

$$\Delta S_m = -R(n_1 \ln \phi_1 + n_2 \ln \phi_2) \quad (2)$$

where n_i is the number of moles of component i with volume fraction ϕ_i. For a system where there are no

† Permanent address: Department of Chemistry, Zhong-Shan University, Guangzhou, People's Republic of China.

0024-9297/86/2219-2765$01.50/0

Table I
Characterization Data for the Polymers Used in Blends

code	polymer	mol % COOH[a]	T_g, °C	M_w[b]	M_n[b]	M_w/M_n
PS_{115}	polystyrene		104	115 000		<1.06
C-37	$C^{4.5}$-PPO	4.5	217	68 700	36 700	1.87
C-34	$C^{6.7}$-PPO	6.7	217	69 200	37 000	1.87
C-29	$C^{8.0}$-PPO	8.0	218	69 500	37 200	1.87
C-33	$C^{10.3}$-PPO	10.3	221	70 100	37 500	1.87

[a] Measured by titration. [b] The molecular mass of carboxylated PPO was calculated by using the GPC data of PPO and $C^{3.0}$-PPO.

specific interactions, ΔG_m decreases with increasing temperature. Therefore, the existence of an upper consolute point (UCST) is predicted. However, the unmodified Flory–Huggins theory does not predict the lower consolute point (LCST) commonly observed in polymer–polymer mixtures. Some newer theories, such as the equation of state and lattice fluid theories, have been presented by Prigogine,[2] Flory,[3] Sanchez and Lacombe,[4] and Simha and Somcynsky.[5] According to these theories, ΔG_m in polymer blends contains three different contributions: the combinatorial entropy of mixing, the exchange interaction and the "free volume term". The combinatorial entropy of mixing in polymers becomes insignificant at high molar masses. The free volume contribution is always positive and increases as a function of temperature. This term leads to the existence of an LCST in polymer–polymer mixtures because of the difference in the thermal expansion coefficients of the pure components. A specific interaction, resulting in a negative exchange interaction contribution to the free energy of polymer mixing, is usually said to be a prerequisite for the miscibility of homopolymer pairs. An increasing number of exceptions to this generalization are being identified, in which at least one of the blend components is a random copolymer. This miscibility phenomenon in the absence of specific interactions has been rationalized on the basis of a mean field, Flory–Huggins type theory.[6-8]

McMaster[9] applied the Prigogine–Flory theory, i.e., the equation of state theory, to polymer–polymer mixtures and demonstrated that a system with a small positive exchange interactional energy parameter, and a very small free volume contribution, can exhibit both UCST and LCST behavior. He also pointed out that such behavior is expected to be rare in polymer–polymer blends.

In practice, the existence of both an UCST and LCST has been established for polymer–solvent systems.[10-12] Schmitt[13] discussed UCST behavior, LCST behavior, and combined UCST and LCST behavior in blends of poly(methyl methacrylate) with poly(styrene-*co*-acrylonitrile). Ueda and Karasz[14] reported the existence of an UCST in chlorinated polyethylene (CPE) blends using the DSC technique. Recently, Inoue[15] found that elastomer blends of *cis*-1,4-polybutadiene and poly(styrene-*co*-butadiene) exhibit both UCST and LCST behavior.

In the present study, we observe that blends of polystyrene (PS_{115}) and carboxylated poly(2,6-dimethyl-1,4-phenylene oxide) (C^y-PPO) copolymers with a degree of carboxylation between 8 and 10 mol % exhibit both UCST and LCST behavior.

Experimental Section

Materials. Polystyrene with M_w = 115 000 (PS_{115}) and narrow molecular weight distribution, M_w/M_n < 1.06, was used as received from Polymer Laboratories, Inc.

Carboxylated poly(2,6-dimethyl-1,4-phenylene oxide) (C^y-PPO) copolymers were prepared as previously described.[16] The sample codes and the characterization data are presented in Table I.

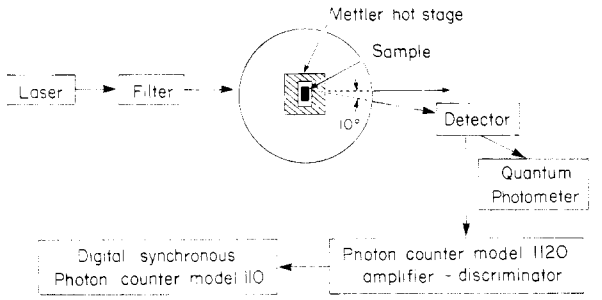

Figure 1. Block diagram of photometric light scattering apparatus.

Blend Preparation. A series of blends of PS and C-PPO was prepared by dissolving appropriate quantities of the pure components in the mixed solvent 5:1 dioxane–toluene, followed by coprecipitation into a large excess of hexane (12:1). The resulting precipitates were dried under vacuum at 90 °C for 3 days.

The films used in light scattering measurements were prepared by dissolving the dried blend powders in toluene containing a small amount of dioxane. This solution (about 1% (w/v)) was cast onto a container with a water surface at 70–80 °C. These cast films were further dried under vacuum at 90 °C for 3 days.

In DSC measurements, the blend powders and compression-molded films yielded the same glass transition temperatures (T_g's).

Measurements. Thermal Analysis. Differential scanning calorimetry experients were conducted with a Perkin-Elmer Model DSC-2. Sample sizes were approximately 20 mg. In the experiments, the blend powder samples were heated at a rate of 20 K/min from 330 to 530 K, rapidly quenched (320 K/min) to room temperature, and scanned at 20 K/min. This process was repeated until a stable T_g was obtained.

An annealing experiment consisted of heating the homogeneous blend sample at a rate of 320 K/min to the selected annealing temperature and maintaining it at this temperature for 20 min. This period was found by experiment to be long enough to attain a distinct phase separation in these samples in the temperature range of interest but not long enough to induce degradation of either component at the highest temperature (320 °C). After annealing, the samples were rapidly quenched to liquid nitrogen temperatures and subsequently scanned at 20 K/min.

Thermogravimetric analysis of blend samples was carried out with a Perkin-Elmer TGS-2 analyzer. The temperature range was from 50 to 900 °C at a scanning rate of 10 °C/min in a nitrogen atmosphere.

Light Scattering Measurements. Phase boundaries were examined by measuring the intensity of scattered light from the sample at an angle of 10° using the photometric light scattering apparatus shown in Figure 1. A film of 0.03–0.04-mm thickness was placed between two glass microscope slides to protect the sample and then mounted in a sample holder located in a Mettler hot stage. The heating rate of the Mettler hot stage can be varied from 0.2 to 10 °C/min. In this experiment, the light scattering intensities were recorded by using a digital synchronous computer photon counter, Model 110 (SSR Instruments Co.).

Results and Discussion

Thermally Induced Phase Separation via DSC. The phase behavior of four miscible blend samples of C^y-PPO/PS_{115} was studied by DSC. The presence of one or two T_g's in the DSC thermograms was used as a criterion for miscibility or immiscibility. The blends were annealed for 20 min at various temperatures above their T_g's but below the decarboxylation temperature of C^y-PPO.[16] Figure 2 shows the glass transition temperatures (T_g, blend) and degradation temperatures ($T_{d,blend}$) as a function of blend composition. The $T_{g,blend}$ values obtained for C^y-PPO/PS_{115} blends are lower than predicted by Fox's equation:

$$\frac{1}{T_{g,blend}} = \frac{W_A}{T_{gA}} + \frac{W_B}{T_{gB}} \quad (3)$$

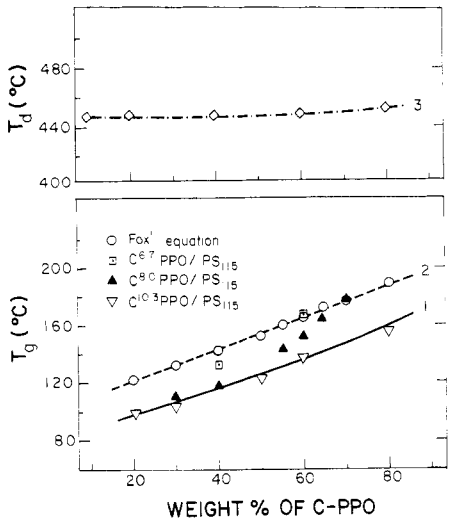

Figure 2. Relationship between T_g (T_d) and blend composition: curve 1, experimental T_g data (guide line through experimental points for $C^{10.3}$-PPO/PS_{115}); curve 2, T_g calculated according to Fox's equation; curve 3, T_d of $C^{10.3}$-PPO/PS_{115} blends vs. blend composition. T_d was taken as the peak of derivative curves in TGA traces.

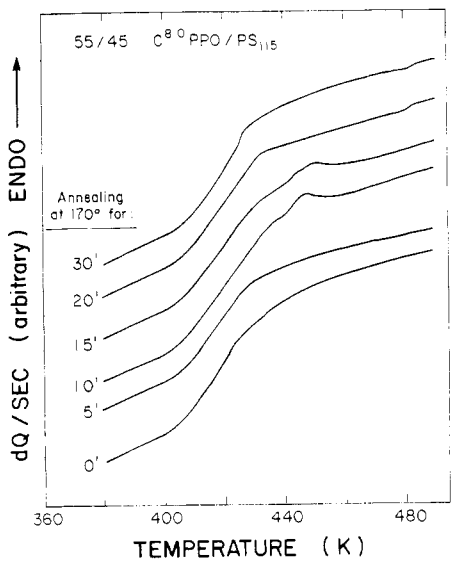

Figure 3. DSC thermograms illustrating the effect of annealing times on phase separation. 55/45 $C^{8.0}$-PPO/PS_{115} blends annealed at 170 °C for various times as shown on the curves.

where T_{gA} and T_{gB} refer to the T_g's of the pure polymers and W_A and W_B are the weight fractions of the blend constituents. This suggests the presence of a specific interaction between C^y-PPO and PS. Such an interaction could play an important role in the phase behavior of the blends.

Figure 3 shows that the phase separation of the samples achieves a stable state within a 20-min annealing period, since the DSC trace shows no further changes upon annealing after this time.

The influence of annealing temperature on C^y-PPO/PS_{115} blends is shown in Figures 4–6. These figures illustrate two different cases: no phase separation induced by the thermal history and the coexistence of an UCST and LCST. For low carboxylation content copolymer blend samples, $C^{4.5}$-PPO and $C^{6.7}$-PPO, the DSC traces (Figure 4) exhibit a series of broadened single T_g's corresponding to various annealing temperatures. No phase separation is observed. For $C^{8.0}$-PPO/PS_{115} (Figure 5) and $C^{10.3}$-PPO/PS_{115} (Figure 6), the effect of thermally induced

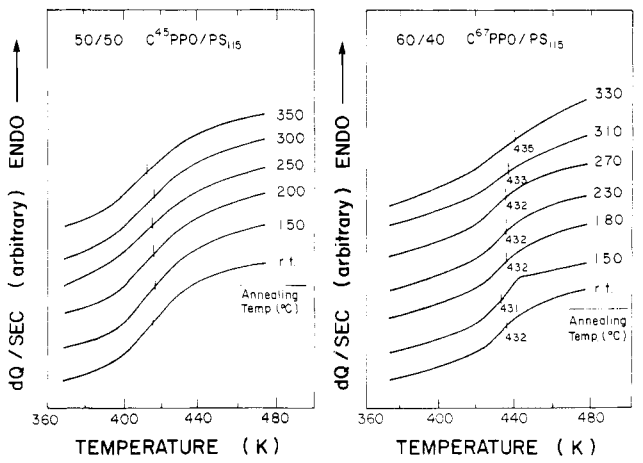

Figure 4. DSC thermograms illustrating phase separation: (left) 50/50 $C^{4.5}$-PPO/PS_{115} blends annealed at different temperatures for 20 min; (right) 60/40 $C^{6.7}$-PPO/PS_{115} blends annealed at different temperatures for 20 min.

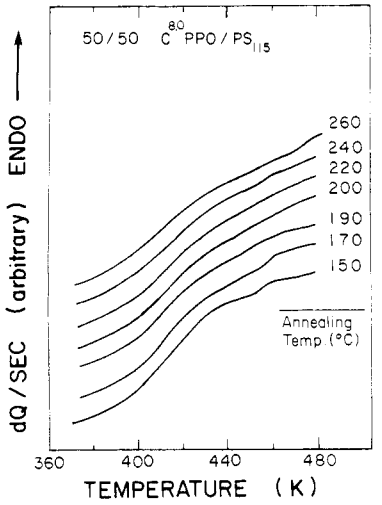

Figure 5. DSC thermograms illustrating phase separation. 50/50 $C^{8.0}$-PPO/PS_{115} blends annealed at different temperatures for 20 min.

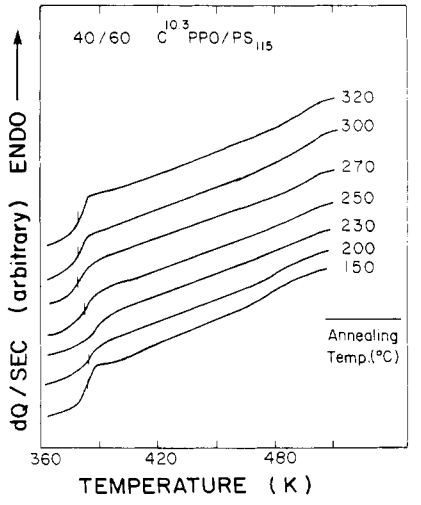

Figure 6. DSC thermograms illustrating phase separation. 40/60 $C^{10.3}$-PPO/PS_{115} blends annealed at different temperatures for 20 min.

phase separation can be seen clearly. The $C^{8.0}$-PPO/PS_{115} system in a ratio of 50/50 displays phase separation at annealing temperatures lower than 200 °C and higher than 250 °C. Between these two temperatures a miscibility region is observed. The behavior of $C^{10.3}$-PPO/PS_{115} is

Table II
Effect of Annealing Temperature on Blend T_g's

		UCST			LCST	
sample	annealing temp, °C	low T_g, °C	high T_g, °C	annealing temp, °C	low T_g, °C	high T_g, °C
40/60 $C^{10.3}$-PPO/PS_{115}	150	110	220	250	108	211
	200	110	211	170	107	227
55/45 $C^{8.0}$-PPO/PS_{115}	160	153	192	250	132	192
	170	152	192	260	132	201
	190	152	191	270	132	207

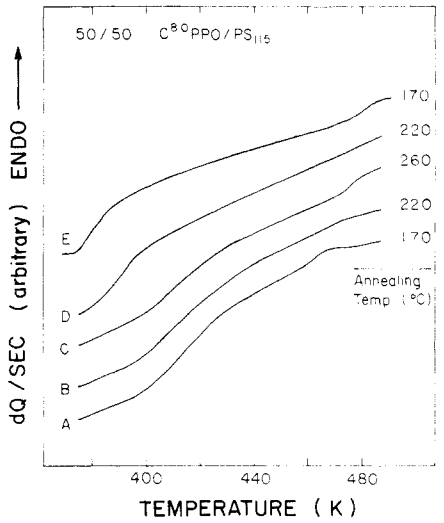

Figure 7. DSC thermograms for 50/50 $C^{8.0}$-PPO/PS_{115} blends showing phase separation is reversible. Curves A, B, C, D, and E are the experimental orders responding to the annealing temperatures of 170, 220, 260, 220, and 170 °C, respectively.

similar to that of the $C^{8.0}$-PPO/PS_{115} sample (Figure 6).

In Table II, the data listed are representative of the two resolved T_g's in the region of phase separation. It is clear that higher carboxyl contents in the copolymer lead to better resolved T_g's. For the $C^{8.0}$-PPO/PS_{115} system, T_g values did not correspond precisely to those of the pure components, 377 and 490 K respectively. This implies that the blends separated to a C^y-PPO-rich phase and a PS-rich phase during the annealing procedure. Moreover, we can see that the phase separation is more distinct in the LCST region than in the UCST region. This result may be attributed to the fact that the UCST is located between the T_g's of the blend components. In the UCST region, PS molecules are more mobile than C-PPO molecules due to the lower T_g of the pure PS component, so the PS domains grow faster than the C-PPO domains during the UCST temperature annealing. But in the LCST region, both PS and C-PPO domains grow at comparable rates. This may be the reason for the more distinct phase separation in the LCST region.

As several sources[17-19] have reported, thermally induced phase separation is easily reversed when the blends are annealed below the respective LCST. In the present study, the changes in transition behavior are completely reversible, as shown in Figure 7. The sample was annealed at 443 K (in the UCST region), cooled rapidly at 330 K, and scanned through 530 K (curve A). It was then annealed in the one-phase region (493 K) and with the same cooling–heating procedure to obtain a homogeneous structure (curve B). By cycling these procedures, the reversed DSC traces were obtained as curves C, D, and E in Figure 7. It is clear that curve E shows a more extreme composition than curve A for the two T_g's. This is attributed to the effect of thermal history on the sample.

The effect of the blend compositions on the phase behavior at the different annealing temperatures is shown

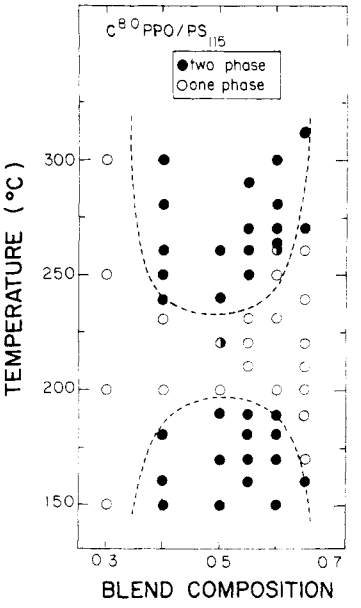

Figure 8. Phase diagram of $C^{8.0}$-PPO/PS_{115} blends. Solid circles indicate that a 20-min annealing period leads to phase separation, and open circles indicate that no phase separation is caused by annealing. Half-filled circles indicate mediate states.

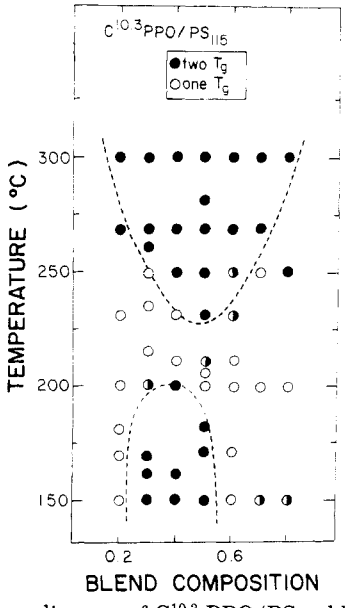

Figure 9. Phase diagram of $C^{10.3}$-PPO/PS_{115} blends.

in Figures 8 and 9. The solid circles indicate that a 20-min annealing period leads to phase separation and the open circles indicate that only one T_g is resolved by DSC and thus no phase separation is observed. From these phase diagrams, the coexistence of an UCST and LCST in C^y-PPO/PS_{115} blend systems where the copolymer contains 8–10.3% degree of carboxylation is evident.

It is obvious that the shapes and locations of these phase diagrams are related to the copolymer composition. Figure

Table III
Temperatures of Phase Boundaries and Critical Points by DSC

	UCST			LCST			
sample	blend comp at boundaries on 160 °C isotherm, wt % C-PPO	crit point, °C	crit comp, wt % C-PPO	blend comp at boundaries on 300 °C isotherm, wt % C-PPO	crit point, °C	crit comp, wt % C-PPO	temp diff between min of LCST and max of UCST, °C
$C^{8.0}$-PPO/PS_{115}	40-65	190	50	40-65	235	50	45
$C^{10.3}$-PPO/PS_{115}	30-50	200	40	20-80	230	50	30

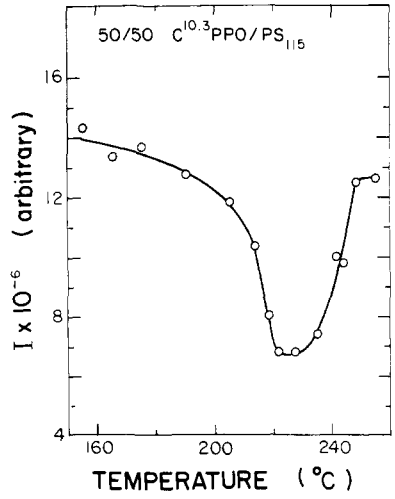

Figure 10. Effect of temperature on scattered light intensity for 50/50 $C^{10.3}$-PPO/PS_{115} blends.

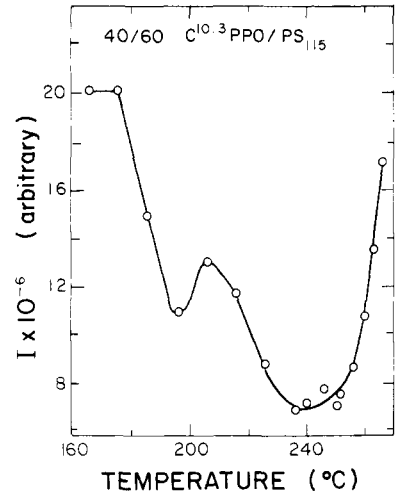

Figure 11. Effect of temperature on scattered light intensity for 40/60 $C^{10.3}$-PPO/PS_{115} blends.

8 shows a two-phase region with a maximum of about 463 K at 50 wt % $C^{8.0}$-PPO, and the blend compositions for the miscibility–immiscibility boundaries on the 160 °C isotherm are between 40 and 65 wt % $C^{8.0}$-PPO. But for the $C^{10.3}$-PPO/PS_{115} system (Figure 9), the maximum temperature occurs at about 473 K at 40 wt % $C^{10.3}$-PPO, and the two-phase region lies between 30 and 50 wt % C-PPO. However, for the LCST behavior, the higher the carboxyl content of the copolymer, the lower the minimum temperature and the wider is the two-phase region at 573 K. The data are listed in Table III. This indicates that the miscible regions between the UCST and LCST depend strongly upon the copolymer composition.

Light Scattering Measurements. To confirm the results obtained from DSC measurements, we determined the temperature dependence of the cloud points in the blend films. The films were annealed at 423 K for 20 min, and the variation of scattered light intensities from the samples was examined while temperature increased at a rate of 2 °C/min.

Three examples of the effect of temperature on the scattered light intensities are shown in Figure 10–12. The cloud point curves were obtained. The regions where relatively little light was scattered suggest single-phase regions. At lower and higher temperatures, there is an increase in scattering intensity, which indicates phase separation.

It is worthwhile to note that the area of lowest scattering intensity examined by light scattering essentially coincided with the single-phase region between the UCST and LCST in the phase diagrams. It should also be noted that the scattering intensities can be reversed by rapidly cooling the sample to room temperature by nitrogen flow and then reheating with a heating rate of 10 °C/min to the desired temperatures. These data are listed in Table IV.

To avoid the deterioration of the samples by long exposure to high temperature during the slow heating process, the highest temperature was limited to below 260 °C. So, for some blend compositions which have LCST temperatures greater than 260 °C, only the UCST was observed.

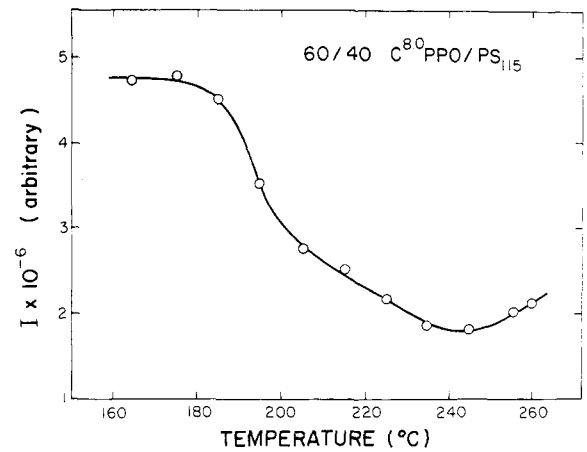

Figure 12. Effect of temperature on scattered light intensity for 60/40 $C^{8.0}$-PPO/PS_{115} blends.

Table IV
Reversibility of Light Scattering for C-PPO/PS Blends

sample	measd order	measd temp, °C	$I \times 10^{-5a}$
60/40 $C^{8.0}$-PPO/PS_{115}	1	230	7.52
	2	170	11.30
	3	230	6.69
60/40 $C^{10.3}$-PPO/PS_{115}	1	200	7.34
	2	225	3.58
	3	238	9.59
	4	200	7.47
	5	225	3.55
	6	240	10.40

[a] Scattering intensity in arbitrary units.

In Figure 11, an increase in intensity appearing around the copolymer T_g may be due to C-PPO molecules passing through their glass transition. Residual strains may be released, causing the sample surface to become irregular, resulting in an increased scattering intensity. This effect can be reduced by annealing above the glass transition temperature of the film and slowly cooling to room temperature to relax any residual strain and stress.

Conclusions

Low carboxyl content ($\lesssim$ 10 mol %) copolymers (C^y-PPO) blended with PS of molar mass 115 000 exhibit a single phase. Phase diagrams for blends of $C^{8.0}$-PPO/PS_{115} and $C^{10.3}$-PPO/PS_{115} exhibit a single-phase region, a UCST, and an LCST. The gap between the UCST and LCST depends on the copolymer composition. For $C^{4.5}$-PPO/PS_{115} and $C^{6.7}$-PPO/PS_{115} blends, no phase separation was observed during thermal treatment because the single-phase region between the UCST and LCST extends beyond the experimental temperature range. The phase separation behavior observed by either DSC or light scattering is reversible.

Acknowledgment. We are grateful to Dr. Hsinjin Yang for help and discussions about the light scattering experiments and to Chris Lantman for his critical reading of the manuscript. We also thank Dr. H. Ueda for many very valuable discussions.

Registry No. PS, 9003-53-6.

References and Notes

(1) Flory, P. J. *Principles of Polymer Chemistry*; Cornell University: Ithaca, NY, 1953.
(2) Prigogine, I.; Bellemans, A.; Colin-Naar, C. *J. Chem. Phys.* **1957**, *26*, 751.
(3) Flory, P. J.; Orwell, R. A.; Vrij, A. *J. Am. Chem. Soc.* **1964**, *86*, 3507.
(4) Sanchez, I. C.; Lacombe, R. H. *J. Phys. Chem.* **1976**, *80*, 2352.
(5) Shimha, R.; Somcynsky, T. *Macromolecules* **1969**, *2*, 343.
(6) Kambour, R. P.; Bendler, J. T.; Bopp, R. C. *Macromolecules* **1983**, *16*, 753.
(7) ten Brinke, G.; Karasz, F. E.; MacKnight, W. J. *Macromolecules* **1983**, *16*, 1827.
(8) Paul, D. R.; Barlow, J. W. *Polymer* **1984**, *25*, 487.
(9) McMaster, L. P. *Macromolecules* **1973**, *6*, 760.
(10) Saeki, I.; Kuwahara, N.; Kaneko, M. *Macromolecules* **1976**, *9*, 101.
(11) Kono, S.; Saeki, S.; Kuwahara, N.; Nakata, M. *Macromolecules* **1975**, *8*, 799.
(12) Izumi, Y.; Mikake, Y. *Polym. J. (Tokyo)* **1972**, *3*, 647.
(13) Schmitt, B. J. *Angew. Chem.* **1979**, *91*, 286.
(14) Ueda, H.; Karasz, F. E. *Macromolecules* **1985**, *18*, 2719.
(15) Inoue, T. *Macromolecules* **1985**, *18*, 2089.
(16) Huang, Y. H.; Cong, G. M.; MacKnight, W. J. *Macromolecules* **1986**, *19*, 2267.
(17) Fried, J. R.; Karasz, F. E.; MacKnight, W. J. *Macromolecules* **1978**, *11*, 150.
(18) Alexandrovich, P.; Karasz, F. E.; MacKnight, W. J. *Polymer* **1977**, *18*, 1022.
(19) Vukovic, R.; Karasz, F. E.; MacKnight, W. J. *Polymer* **1983**, *24*, 529.

Osmotic Pressure of Star and Ring Polymers in Semidilute Solution

Binny J. Cherayil,[†] M. G. Bawendi,[†] Akira Miyake,[‡] and Karl F. Freed*[†]

The James Franck Institute and the Department of Chemistry, The University of Chicago, Chicago, Illinois 60637, and International Christian University, 10-2 Osawa 3-chome, Mitaka, Tokyo, Japan. *Received April 11, 1986*

ABSTRACT: The conformational space renormalization group method is used to calculate the osmotic pressure of semidilute solutions of star and ring polymers in marginal to good solvents to first order in ϵ, where $\epsilon = 4 - d$ and d is the spatial dimension. The results are expressed in terms of an experimentally measurable reduced concentration variable $c/c^* = c\langle A_2\rangle_w M_n$, with $\langle A_2\rangle_w$ the weight-averaged second virial coefficient and M_n a number-averaged molecular weight. The osmotic pressure is found to scale with the same power of the concentration for both stars and rings in the semidilute region, in agreement with scaling theory and asymptotic analyses, but there are fairly large differences in the values of the prefactor coefficients between different polymer types. This is in contrast to the predictions of scaling and of an approximate analytic evaluation of the osmotic pressure, which yields a single universal curve for these two architectural classes of polymer. Criteria are also provided for the onset of semidilute solution power law behavior as a function of the reduced concentration and solvent quality.

I. Introduction

Star and ring polymers constitute an important class of polymers whose study helps clarify the connection between polymer physical properties and molecular architecture. While there is a fairly extensive body of experimental and theoretical literature that explores this connection for the case of polymers at infinite dilution,[1-5] there have been fewer studies at concentrations where overlap between different chains becomes important.[6-9] However, these studies of semidilute solutions have focused only on linear polymers, and the question of whether topological differences significantly influence the large-scale properties of semidilute polymer solutions has so far only been addressed by scaling methods.[10-12] Scaling argues that polymer properties like the osmotic pressure must become independent of the molecular weight in semidilute solution, and, consequently, linear, star, and ring polymers scale in the same manner. Whether or not a full theory predicts differences and the extent to which such differences represent measurable effects is not yet known. Nor is it known whether the scaling functions for different polymer architectures in semidilute solution can be represented in terms of a single universal curve.

In this paper we examine the role of polymer architecture in influencing semidilute solution properties by calculating the osmotic pressure of dilute through semidilute solutions of star and ring polymers in marginal to good solvents to order ϵ, where $\epsilon = 4 - d$ and d is the spatial

[†] The University of Chicago.
[‡] International Christian University.

0024-9297/86/2219-2770$01.50/0